PHYSICAL REVIEW A VOLUME 36, NUMBER 11 DECEMBER 1, 1987

Simplified models of electron excitation and ionization at very high E/n

A. V. Phelps* and B. M. Jelenković†
Joint Institute for Laboratory Astrophysics, University of Colorado and National Bureau of Standards, Boulder, Colorado 80309-0440

L. C. Pitchford
GTE Laboratories, Inc., Waltham, Massachusetts 02254
(Received 7 July 1987)

Models of electron excitation and ionization at very high electric-field–to–gas-density ratios E/n are compared under conditions appropriate to discharge experiments at low gas densities, such as those in N_2 described in the preceding paper. The models considered use the monoenergetic beam approximation in a velocity moment technique for solution of the electron Boltzmann equation. They differ in the treatment of the electrons produced by ionization and in the use of either the momentum balance or the energy balance to obtain the effective frictional effect. A simplified single-beam model is found to agree reasonably well with multiple-beam models, with the few published Monte Carlo results, and with experimentally measured spatial ionization coefficients.

I. INTRODUCTION

The objective of this work is to develop simple, first-order models of electron motion applicable from moderate to very high electric-field (E) to gas-density (n) ratios and suitable for use in the analysis of experimental data such as that presented in the preceding paper.[1] At moderate E/n the models to be presented describe the transition from an initial nonequilibrium motion in which there are few collisions with the gas molecules and essentially free-fall acceleration of the electrons to the hydrodynamic or equilibrium motion in which there is a balance between the energy and momentum gained from the electric field and lost in collisions. At very high E/n the models describe the runaway electron motion in which collisional equilibrium in the presence of the electric field is never reached and yet the electron current resulting from collisional ionization of the gas eventually grows exponentially with distance. Since the previous experiments and theory of electrons at very high E/n have been reviewed in I, we will consider here only the previous work particularly relevant to the present models. Here and in the remainder of this paper Ref. 1 will be referred to as I. The models described here have also been used in preliminary analyses[2] of emission resulting from electron excitation of H_2 and Ar at very high E/n.

Theories of electron motion in spatially uniform electric fields at very high E/n which have yielded results suitable for analysis of experiments can conveniently be divided into solutions of the collisional Boltzmann equation and Monte Carlo simulations of the experiment. Approximate solutions of the electron Boltzmann equation for very high E/n when electron energy losses can be neglected were obtained by Stuart and Gerjuoy[3] and, more recently, by Briggs and Yu,[4] by Friedland and Kagan,[5] and by Lagushenko and Maya.[6] Energy losses were included in the analysis of runaway in weakly ionized gases by Gurevich.[7] The moment technique was applied to the solution of the nonequilibrium Boltzmann equation by Müller and co-workers[8] and has been applied more recently by Ingold[9] and by Friedland and Kagan.[5] Riemann[10] has investigated electron motion in the E/n range between moderate and very high E/n. Iterative solutions of the full nonequilibrium Boltzmann equation have recently been carried out by Pitchford, Moratz, Segur, and Yousfi,[11] but results are available only for isotropic scattering models. In view of the increasing importance of anisotropic scattering with increasing E/n found in N_2 by Phelps and Pitchford,[12] results obtained assuming isotropic scattering must be regarded as preliminary.

Monte Carlo techniques have been applied to the calculation of electron multiplication at very high E/n by several authors.[13–19] The results of Parker *et al.*[13] are in a form suitable for comparison with our models. The model of Granzow and McClure[14] is for E/n at the upper limit of those considered in the present paper. Folkhard and Haydon[15] and Tagashira and co-workers[16] applied Monte Carlo techniques to studies of electron motion and ionization at the lower E/n values of interest here. Hayashi[17] considered current growth at these E/n in He and H_2. Lauer *et al.*[18] present time-dependent results. The results of Moratz, Pitchford, and Bardsley[19] are currently being extended to realistic anisotropic scattering.

In this paper we will consider in detail only models of electron motion based on the moment method of solution of the Boltzmann equation. Thus, in Sec. II we first derive equations describing the behavior of an electron beam. These relations are then used to predict the spatially dependent current growth and excitation coefficients for the single-beam models in Sec. II B. In Sec. II C the single-beam results are used to build a mul-

tibeam model. Predictions of the various models are compared in Sec. III.

II. ELECTRON-BEAM MODELS

The steady-state Boltzmann equation in one spatial dimension for electrons in a cold gas can be written as[20]

$$\nabla_r \cdot \mathbf{v} f(v,\theta,z) - \frac{e\mathbf{E}}{m} \cdot \nabla_{\mathbf{v}} f(v,\theta,z) = -n \sum_k 2\pi v f(v,\theta,z) \int I^k(v,\psi) \sin\psi \, d\psi + n \sum_k 2\pi v \int d\theta' f(v',\theta',z) I^k(v',\psi) \times \sin\theta' (v'/v)^2 dv'/dv \ , \quad (1)$$

where e and m are the charge and mass of the electron, v' and v are the electron speeds before and after the collision, $I^k(v',\psi)$ is the differential cross section for scattering of an electron through an angle $\psi=\theta-\theta'$ in process k, $f(v,\theta,z)$ is the electron velocity distribution, and n is the gas density. In Eq. (1) the relation between v' and v depends upon whether the collision is elastic or inelastic.[20] We consider an electron-velocity distribution that can be approximated by that of a monoenergetic beam moving in the direction of electron acceleration, i.e., $f(v,\theta,z)=n_e(z)\delta(v-u(z))\delta(\theta)(2\pi N^2 \sin\theta)^{-1}$, where u is velocity of the beam electrons at z. The validity of this approximation will be discussed in Sec. III. Integration of the first three velocity moments of Eq. (1) over velocity space yields[8,9] the particle number balance,

$$\frac{d(un_e)}{dz} = uQ_0^i(u) n_e n \ ; \quad (2)$$

the momentum balance,

$$\frac{d(n_e u^2)}{dz} = \frac{eEn_e}{m} - n_e u^2 n \sum_k Q_m^k(u) \ ; \quad (3)$$

and the energy balance,

$$\frac{1}{2}\frac{d(n_e u^3)}{dz} = \frac{ueEn_e}{m} - \frac{n_e u n}{2} \sum_{k>0} u_k^2 Q_0^k(u) - \frac{m}{M} n_e n u^3 Q_m^0(u) \ , \quad (4)$$

where $Q_m^k(u)$ is the momentum-transfer cross section for collision process k defined by Ecker and Müller[8] and considered in more detail by Phelps and Pitchford,[12] $n_e(z)$ is the electron density, $Q_0^i(u)$ and $Q_0^k(u)$ are the total ionization and excitation cross sections, $Q_m^0(u)$ is the elastic momentum-transfer cross section, M is the mass of the gas atoms or molecules, and u_k is the electron velocity at the excitation threshold ($\varepsilon_k = mu_k^2/2$). Here the cross-section notation is that of Ref. 12. Note that the summation in Eq. (3) includes elastic momentum-transfer collisions, whereas that in Eq. (4) does not include elastic scattering. Both sums include ionization.

The electron density is next eliminated from Eqs. (3) and (4) using Eq. (2) so as to obtain differential equations for u from the momentum balance

$$\frac{1}{2}\frac{du^2}{dnz} = \frac{eE}{mn} - u^2 \sum_k Q_m^k(u) - u^2 Q_0^i(u) \quad (5)$$

and from the energy balance

$$\frac{1}{2}\frac{du^2}{dnz} = \frac{eE}{mn} - \sum_k \frac{u_k^2}{2} Q_0^k(u) - \frac{2m}{M}\frac{u^2}{2} Q_m^0(u) - \frac{u^2}{2} Q_0^i(u) \ . \quad (6)$$

For electrons created at z_0 with negligible initial velocity in the z direction, these equations yield for the momentum balance

$$nz - nz_0 = \int_0^{\varepsilon} d\varepsilon' \frac{1}{\left[(eE/n) - 2\varepsilon' \sum_k Q_m^k(\varepsilon') - 2\varepsilon' Q_0^i(\varepsilon')\right]} \quad (7)$$

and for the energy balance

$$nz - nz_0 = \int_0^{\varepsilon} d\varepsilon' \frac{1}{\left[(eE/n) - \sum_k \varepsilon_k' Q_0^k(\varepsilon') - (2m/M)\varepsilon' Q_m^0(\varepsilon') - \varepsilon' Q_0^i(\varepsilon')\right]} \ , \quad (8)$$

where $\varepsilon = mu^2/2$. As discussed by several authors[7-10] for the case of no ionization growth, the condition that the electric field term of Eq. (5) or of Eq. (6) balances the collision terms is the condition for a constant electron drift velocity. Runaway is said to occur when the electron velocity continuously increases with z for all $z > z_0$, i.e., the electric field term exceeds the collision terms.

Equations (2) and (7) or (2) and (8) model the spatially dependent behavior of the electron density, current, and velocity or energy as that of a monoenergetic beam of electrons which is constrained to move in the direction of the acceleration due to the electric field. The effects of collisions and the production of new electrons by ionization are treated as friction terms. Since at high electron energies the contribution of inelastic collisions to $2\varepsilon \sum_k Q_m^k(\varepsilon)$ in Eq. (7) is approximately equal[12] to $\sum_k \varepsilon_k Q_0^k(\varepsilon)$ in Eq. (8), the contributions of inelastic collisions to the effective friction or drag is nearly the same for both the energy- and momentum-balance equations. Because of the $2m/M$ factor in Eq. (8), the contribution of elastic collisions to the frictional effect for the energy balance is negligible for the conditions of interest here. On the other hand, elastic collisions are the largest contribution to the frictional effect for the momentum-

balance equation, e.g., for N_2 at 10^4 eV the elastic contribution to Eq. (7) is twice the inelastic contribution.[12] The momentum- and energy-balance equations also differ in the contributions of ionization growth to the friction. These friction terms represent the new electrons being introduced into the beam at either the beam velocity squared [Eq. (5)] or at the beam energy [Eq. (6)]. Because of the factor of two in Eq. (7), ionization results in a greater effective friction in the momentum-balance case. Since a monoenergetic beam is completely described by two parameters, i.e., the density and the velocity or the energy, our one-dimensional monoenergetic beam model forces us to choose either the momentum balance or the energy balance to describe the average v^2 of the electrons. The two solutions are not equivalent. In previous work, Müller[8] chose the momentum balance while Friedland[5] chose the energy balance. We will discuss results from both choices in Secs. II A and II B.

A. Single-beam models

Equations (2) and (5)–(8) are next used to construct "single-beam" models of electron motion. When Eq. (5) or Eq. (7) is applied to the calculation of the electron energy as a function of position and Eq. (2) is used to calculate the electron density, the model will be called the momentum-balance, single-beam model. Similarly, Eq. (6) or (8) and Eq. (2) are the primary equations for the energy-balance, single-beam model. These models are a simplification of the model of Ingold[9] in that we assume that the "random speed" is negligible compared to the drift speed. In the present models the electrons originate at the cathode, i.e., $z_0=0$ in Eqs. (7) and (8), so that $nz(\varepsilon)$ or $\varepsilon(nz)$ can easily be calculated using, for example, cross-section data for N_2 from Ref. 12. Note that because of the presence of the $Q_0^i(\varepsilon)$ term in the denominator of Eqs. (7) and (8) and the variation[12] of $Q_0^i(\varepsilon)$ as $(1/\varepsilon)\ln\varepsilon$ at high ε, the electric field term cannot exceed this ionization-growth term and the runaway phenomena will not occur.

The spatial excitation (ionization) coefficient $\alpha^k(z)$ for electrons is obtained using the excitation (ionization) cross section $Q_0^k(\varepsilon)$ and the energy-distribution function for the electron beam. Thus,

$$\frac{\alpha^k(z)}{n}=\frac{\int_0^\infty vQ_0^k(v)f(v,\theta,z)d^3v}{\int_0^\infty v\cos\theta f(v,\theta,z)d^3v}=\frac{\int_0^\infty v^3Q_0^k(v)\delta(v-u(z))dv}{\int_0^\infty v^3\delta(v-u(z))dv}=Q_0^k(u(z))\ . \tag{9}$$

The current growth is obtained by noting that $j_e(z)=en_e(z)u(z)$ and integrating Eq. (2) to obtain

$$\frac{j_e(z)}{j_e(0)}\equiv M(z)=\exp\left[\int_0^z nQ_0^i(u(z))dz\right]=\exp\left[\int_0^{\varepsilon=eEz} nQ_0^i(\varepsilon)\left[\frac{dz}{d\varepsilon}\right]d\varepsilon\right]\ . \tag{10}$$

Here $j_e(0)$ is the electron current leaving the cathode and $M(z)$ is the electron current multiplication. The change of variables in the integrals of Eq. (10) is possible because in this single-beam approximation the electron energy is a unique function of the distance from the cathode as given by Eq. (7) or (8). From Eq. (6) of I and the accompanying discussion in I, it will be recalled that the experiment yields an "apparent excitation coefficient" defined by $\beta^k(z)/n=[\alpha^k(z)/n][j_e(z)/j_e(d)]$ when electron excitation is dominant. The experimental quantities can thus be determined very simply from Eqs. (9) and (10) with either Eq. (7) or Eq. (8) to determine the beam energy. The very simple forms of Eqs. (7)–(10) allow one to calculate $\alpha^k(z)/n$ and $j_e(z)/j_e(0)$ for a wide variety of E/n, nd, and cross sections. Comparisons with other models will be made in Sec. III.

These single-beam models, when suitably modified to take into account the near equality of the ion and neutral masses, also offer a basis for estimating the role of ions in the production of excited species, e.g., the production of excited N_2 by fast N^+ in I. These considerations will not be presented in this paper.

B. Multiple-beam models

As a next level of approximation we consider here multiple-beam models introduced by Müller and co-workers[8] and extended by Friedland and Kagan[5] in which the secondary electrons are treated more rigorously. Thus, each secondary is treated as a new and distinct beam which individually obeys particle-conserving moment equations; i.e., $Q_0^i(\varepsilon)=0$ in the ionization growth terms in Eqs. (2) and (5)–(8). Ionization is retained in the summations appearing in these equations. In this model, each individual beam is monoenergetic, but the ensemble average is a sum over the many individual beams. In contrast to the single monoenergetic beam model, a spread in energy is introduced by each ionization event in the multiple-beam formulation. This model is close in spirit to particle simulations where many individual particle trajectories are calculated and sums over the individual particle yield the macroscopic averages. In the multiple-beam model, however, the detailed tracking of the individual beams and the summations is handled analytically. At high E/N where the production of secondary electrons is the primary reason for spread in the beam energy, this model is expected to be quite good.

The multiple-beam model introduced by Müller and co-workers[8] assumes that each electron leaving the cathode or produced by ionization of the gas is produced with zero initial energy and obeys the momentum balance given by Eq. (3). Thus,

$$\frac{d\varepsilon}{dnz}=\frac{eE}{n}-2\varepsilon\sum_k Q_m^k(\varepsilon) \tag{11}$$

and

$$nz-nz_0=\int_0^\varepsilon d\varepsilon'\frac{1}{\left[(eE/n)-2\varepsilon'\sum_k Q_m^k(\varepsilon')\right]}\ , \tag{12}$$

where the summation includes elastic scattering ($k=0$),

excitation, and ionization ($k=i$). The application of an E/n greater than the maximum value of $2\varepsilon\sum_k Q_m^k(\varepsilon)$ results in electron runaway. At sufficiently large $E/(n\sum_k Q_m^i)$ the runaway motion approaches that of free fall in the accelerating electric field as discussed in Sec. II C.

Müller[8] assumed that the electric field is spatially uniform and obtained the spatial dependence of the current density in the form of the integral equation

$$\frac{j_e(z)}{j_e(0)} \equiv M(z) = 1 + \int_{z_0=0}^{z} nQ_0^i(z_0)M(z-z_0)dz_0 \ . \tag{13}$$

Laplace transform[5,7] and iteration[21] techniques have been applied to the solution of this equation.

When the multiplication $M(z)$ is large compared to unity, as at large z, the solution[3,4,6] to Eq. (13) is $M(z)=\exp(\alpha_i z)$, where α_i is the spatial ionization coefficient.[12,15,20] Here and elsewhere α_i is distinguished from $\alpha_i(z)$, since α_i is independent of z. In this limit Eq. (13) can be written as

$$1 = \int_{\varepsilon_i}^{\varepsilon_0} Q_0^i(\varepsilon)\exp[-(\alpha_i/n)nz(\varepsilon)]\frac{d(nz)}{d\varepsilon}d\varepsilon \ , \tag{14}$$

where $d\varepsilon/d(nz)$ and $nz(\varepsilon)$ are as given by Eqs. (5) and (7) with Q_0^i and z_0 set to zero and u^2 replaced by $u^2=2\varepsilon/m$. Here ε_0 is the smaller of infinity or the energy at which the right-hand side of Eq. (5) goes to zero. If, in addition, the E/n is large enough so that momentum and energy losses are small so that the electrons undergo free-fall motion ($\varepsilon=eEz$), then Eq. (14) becomes[4-6]

$$eE/n = \int_0^{\infty} Q_0^i(\varepsilon)\exp(\eta\varepsilon/e)d\varepsilon \ , \tag{15}$$

where $\eta=\alpha_i/E$ is the number of ionization events per volt. As pointed out by several authors,[4-8] this spatial ionization growth coefficient is independent of position even though the electron is in free-fall motion, i.e., a repeated time history for each new electron leads to exponential growth. Various authors have considered the corresponding growth in time.[3,4] In the limit of $M\rightarrow 1$ and small energy loss, Eq. (13) can be written as

$$\ln M(z) = \frac{n}{eE}\int_0^{eV(z)} Q_0^i(\varepsilon)d\varepsilon \ , \tag{16}$$

where eV is the energy of the electrons in the absence of collisions. This limit was considered by Dempster[22] and will be used in Sec. III.

Müller[8] also solves for the electron velocity distribution and obtains

$$\frac{f(v,z)}{j_e(0)} = \frac{\delta[v-u(z)]}{u(z)} + \left[\frac{eE}{mn} - v^2\sum_k Q_m^k\right]^{-1}\frac{\partial M[nz-Y(v)]}{\partial(nz)} \ , \tag{17}$$

where $Y(v)$ is the right-hand side of Eq. (7) expressed in terms of the electron velocity. Here the first term represents electrons which were produced at the cathode while the second term represents electrons produced by impact ionization, i.e., the secondary and subsequent electrons. The zeroth and first velocity moments of Eq. (17) yield the electron density and the convective velocity for the electrons.

The excitation coefficients for this model are obtained by substituting Eq. (17) into the first form of Eq. (9). The first term in Eq. (17) leads to an excitation coefficient equal to $j_e(0)Q_0^k(u)/j_T$. The contribution of the second term in Eq. (17) is very complicated and must be evaluated numerically.

A useful limit to the excitation coefficient applies at very high E/n where the electron motion can be approximated by free fall and where the distribution in energy of the secondary electrons is broad compared to the energy range over which the excitation cross section is significant, e.g., for excitation of a triplet state of N_2. In this limit the excitation coefficient due to secondary electrons $\alpha_{\rm sec}^k$ is obtained by substituting Eq. (17) into Eq. (9) and is given by

$$\frac{\alpha_{\rm sec}^k(z)}{n} = \frac{\alpha_i(z)}{n}\frac{n}{eE}\int_{\varepsilon_k}^{\infty} Q^k(\varepsilon)d\varepsilon \ . \tag{18}$$

As an example of the application of this result, we note that using the cross sections of Ref. 12 the integral in Eq. (18) is 70 eVm^2 for the $C\,^3\Pi_u$ state and 170 eVm^2 for the $B\,^3\Pi_g$ group of states. These results lead to very small excitation coefficients compared to ionization coefficients at high E/n. See Fig. 12 of I. This effect results from the rapid acceleration of the low-energy secondary electrons produced by ionization through the energy range in which the excitation is significant. Thus, in this high-(E/n) limit, secondary electrons are much less effective in the excitation of optically forbidden transitions than when a high-energy electron beam passes through a gas, e.g., nitrogen,[23] in the presence of a low or zero E/n.

Friedland and Kagan[5] have solved for the current growth using the second velocity or energy moment equation, Eq. (4), to determine the motion of the electron beams. They treated the electrons produced by ionization by an integral-equation method similar to that of Müller and co-workers.[8] Their work was directed toward the derivation of analytic relations for the ionization coefficients in nonuniform as well as uniform electric fields. A comparison with some of their results will be made in Sec. III C. They also considered the exponential growth and free-fall limits which were discussed in connection with Eqs. (14) and (15).

C. Range of application of limiting solution

In this section we consider the range of E/n and nz values in which the various approximations used in Secs. II A and II B are expected to be valid. The results are summarized in Fig. 1 where we have plotted curves of nz versus E/n for the various transitions. The diagonal lines give the energy an electron would acquire in the distance nz under the action of the electric field in free fall, i.e., the energy available from the field in going from the cathode to z. Also shown are points representing the E/n and nd values for which measurements of N_2 emis-

sion were reported in I. In modeling these constant E/n discharges one must consider all nz less than the experimental nd.

For the purposes of this discussion we will define the transition from free-fall motion of an electron to a drift motion to occur when the energy which an electron starting at a low energy would gain in the absence of collisions equals the steady-state or equilibrium energy, i.e., the energy at which the acceleration by the electric field balances the frictional effect of collisions or when the denominator of Eq. (7), (8), or (12) equals zero. In the case of one of the beams of the multibeam, energy-balance solution, this "energy-relaxation limit" occurs when

$$\frac{eE}{n}=\sum_{k>0}\varepsilon_k Q_0^k(\varepsilon a)+\frac{2m}{M}\varepsilon_a Q_m^0(\varepsilon_a)\ , \tag{19}$$

where $\varepsilon_a=(nz)(E/n)$ is the energy available from the electric field at z under free-fall conditions. Using the N_2 cross sections of Ref. 12, we obtain the solid curve of Fig. 1. This calculation shows that electrons injected with an energy of a few eV into a region where E/n is between 100 and 800 Td will gain energy as though in free fall until they have traversed a column density of about 5×10^{19} m^{-2}. (1 Td$\equiv10^{-21}$ V m^2.) At nz several times this value the electrons begin a drift motion in which the gain in energy from the field is balanced by the loss of energy in collisions, i.e., an equilibrium or hydrodynamic motion.[24] The vertical portion of the curve indicates that for E/n greater than about 950 Td the electrons will undergo runaway[7,8] and so never relax to energy equilibrium with the electric field. For simplicity, we have omitted the portion of the curve given by Eq. (19) for nz greater than 2×10^{20} m^{-2} for which nz increases with decreasing E/n. This curve applies to electrons which somehow reach high energies and shows[8,10] that electrons with sufficient initial energy can undergo energy runaway at E/n below 950 Td in N_2.

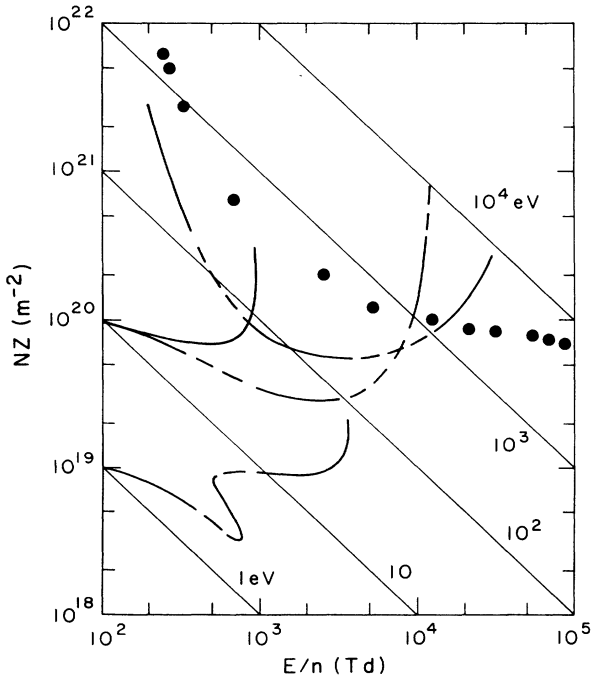

FIG. 1. Curves marking the transition from regions of applicability of various approximations developed in Sec. II. The solid curve and single link chain curves mark the energy relaxation and momentum relaxation transition, while the double link curve is calculated using the single-beam, energy-loss model with ionization growth. The triple link chain curve is calculated from the condition $\alpha_i z=1$. The points are values of nd vs E/n from the experiments with N_2 discussed in I.

The single-link chain curve of Fig. 1 shows the E/n versus nz curve for the transition from free fall to drift motion when the momentum balance is used to describe the motion of one of the beams of the multibeam solution, i.e., when the denominator of Eq. (12) is set equal to zero in order to evaluate ε_a. This transition will be referred to as the "momentum-relaxation" transition or limit. The structure in the curve near $\varepsilon_a=2$ eV is caused by the well-known resonance in electron scattering by N_2 at that energy.[12] This curve shows that for $E/n<3000$ Td free-fall motion with respect to momentum-transfer collisions occurs only for nz less than about $5\times10^{18}m^{-2}$ or an order of magnitude less than for the energy-limited case. We note that momentum runaway occurs at an E/n of about 3700 Td or about four times that for energy runaway. Note also that the different nz values for the momentum-relaxation and energy-relaxation limits are evident in the calculations of the overshoot of the convective velocity of electrons in a spatially varying electric field.[19]

The double chain curve marks the transition between free fall and drift motion as determined from the single-beam, energy-balance model. The curve never becomes truly vertical with the result that although the electron energy becomes very large at very high E/n there is never runaway in the conventional sense.

The triple link chain curve marks the transition from the condition of small ionization, $M-1\ll1$, to the condition of large ionization growth where $M(z)=\exp(\alpha_i z)\gg1$, as required for the validity of Eqs. (14) and (15). The curve is calculated using $(\alpha_i/n)(nd)=1$, where the α_i/n values are from experiment for $E/n<800$ Td and from the multibeam, energy-balance model for higher E/n. For nz significantly below this ionization growth transition and below or to the right of the energy-based free-fall transition, Eq. (16) is valid.

D. Backscattered electrons

In this section we consider the modifications to the single-beam formulas which we have used in a first-order investigation of the excitation and ionization caused by electrons which are backscattered from the anode. Even though the models of backscattering presented here are very elementary, they provide a means for semiquantitative comparison of theory and this very important process in very high E/n discharge experiments. A detailed treatment of the almost identical problem for 120-keV

electrons injected into a gas in the presence of an opposing electric field has been carried out by Smith[25] using Monte Carlo techniques. We will limit the present discussion to relationships based on the energy balance as given in Eq. (6). An electron of energy ε_r leaving the anode will be subject to the effects of the opposing electric field as expressed by reversing the sign of the first term on the right-hand side of Eq. (6), i.e., the field term in Eq. (4) is really the scalar product of **u** and **E**. It is convenient to measure the electron position by its distance, $x=d-z$, from the anode. In this initial investigation the electrons are assumed to be emitted normal to the anode plane. This distance is obtained by integrating the modified Eq. (6) to obtain

$$nx=\int_{\varepsilon}^{\varepsilon_r} d\varepsilon' \frac{1}{\left[\pm(eE/n)+\sum \varepsilon_k Q_0^k(\varepsilon')+(2m/M)\varepsilon' Q_m^0(\varepsilon')+\varepsilon' Q_0^i(\varepsilon')\right]}, \tag{20}$$

where ε is the electron energy at x. Here the + sign applies when the electron is leaving the anode and the − sign applies when the electron is returning to the anode. We are concerned with the excitation and ionization produced as the electron slows down and as it accelerates again and so use $\varepsilon(nx)$ calculated from Eq. (20) to calculate $\alpha^k(x)/n$ from Eq. (9).

Parker and co-workers[13] included the effects of repeated reflections of an electron at the anode. In the free-fall limit, the effect of backscattering is to increase the ionization by twice that for the first crossing times the probability of the reflection. When summed, repeated reflection at the anode increases the total ionization by $(1+r)/(1-r)$, where r is the backscattering or reflection coefficient. Again it is assumed the electrons are emitted normal to the anode plane and that the angular deflection of the electrons by collisions is omitted. We expect that in the more accurate solutions of this problem, the angular deflection on scattering will be of significantly reduced importance because of the spread in angle of electrons leaving the anode.

III. COMPARISONS OF MODELS

In this section we will compare ionization coefficients, multiplication factors, and slowing-down behavior calculated for electrons using various models discussed in Sec. II. Experiments will be compared with the models where available. These comparisons and the comparisons of calculated and measured excitation coefficients made in I will be used to draw tentative conclusions as to the utility of our single-beam model. Final conclusions will have to await the availability of more detailed models and experiments for a wide range of parameters.

A. Apparent ionization coefficient

The first comparison is of the apparent ionization coefficients for H_2 calculated by Müller[8] using his multibeam, momentum-balance model and as calculated using our single-beam, momentum-balance model. The apparent ionization coefficient used by Müller is the number of ionization events per unit distance in the field direction per electron leaving the cathode. The present analysis is basically a comparison between two approximate methods of accounting for the effects of ionization growth on the behavior of the electrons. Thus, the smooth curves of Fig. 2 show the apparent ionization coefficients from Fig. 8(a) of Müller[8] plotted as a function of the energy available to the electron as it moves from the cathode to a point z, i.e., $\varepsilon_a=e(E/n)nz=eV(z)$. The points show our calculations using the momentum-balance version of the single-beam model. The beam energy versus z was calculated using Eq. (7) with $z_0=0$ and $\sum_k Q_m^k(\varepsilon)=Q_1(\varepsilon)$ from Müller,[8] and Eqs. (9) and (10) were used to calculate $\alpha_i(z)$ and $j_e(z)$. Note that in Fig. 1 the apparent ionization coefficients $\beta_c^i(z)/n$ are normalized to the cathode current density rather than to the total current density as in I, i.e.,

$$\frac{\beta_c^i(z)}{n}\equiv\frac{\alpha^i(z)}{n}\frac{j_e(z)}{j_e(0)}. \tag{21}$$

From Fig. 2 we see that the agreement between the

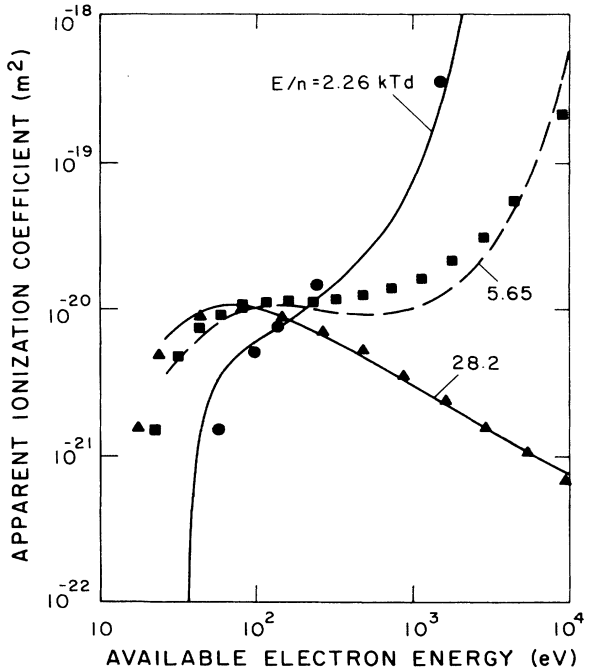

FIG. 2. Comparison of calculated apparent ionization coefficients vs the available energy using the multiple-beam model (smooth curve) and using the single-beam model (points). Both calculations used the momentum-balance approximation and the effective momentum-transfer cross section from Müller (Ref. 8).

two models is excellent at $E/n = 28.2$ kTd. This agreement is expected since collisions are so infrequent that the electron energy is very nearly equal to the available energy (free fall) and since at these relatively small nz electron avalanching is negligble. Thus $\beta_c^i(z) \approx Q_0^i(eEz)$. At the lower E/n the agreement between the two models is quite satisfactory considering the simplicity of the single-beam model. At these E/n collisional effects are large enough so that with momentum-balance models the electrons reach an equilibrium drift at sufficiently large nz. From this comparison we conclude that for the range of E/n and nz considered, the effects of ionization on the momentum balance can be treated approximately equally well by including a friction term or by considering beams of secondary electrons.

B. Electron multiplication

In Fig. 3 we compare values of the electron multiplication M calculated using our single-beam model with the Monte Carlo calculations of Parker and co-workers.[13] We have chosen to plot values of $\ln M$ as a function of the available electron energy because this allows us to show a wide range of M values and because an exponential growth becomes a straight line on this log-log plot. The Monte Carlo results shown by the solid points were calculated[13] using a model in which only ionizing collisions were considered. The open points were obtained from the Monte Carlo results (solid points) by dividing by the correction for backscattering discussed in Sec. II D. The reflection coefficients used are those of Parker and co-workers, i.e., 0.1 for 2.8 kTd and 0.3 for 90 kTd. We see that the open points are in good agreement with the results of our single-beam models for the range of E/n and available energy shown. For $E/n > 90$ kTd the values of M calculated using Eq. (10) and $dz/d\varepsilon$ values from either the energy-balance or momentum-balance approximations are only slightly larger than for the free-fall model, i.e., the free-fall model is a good approximation.

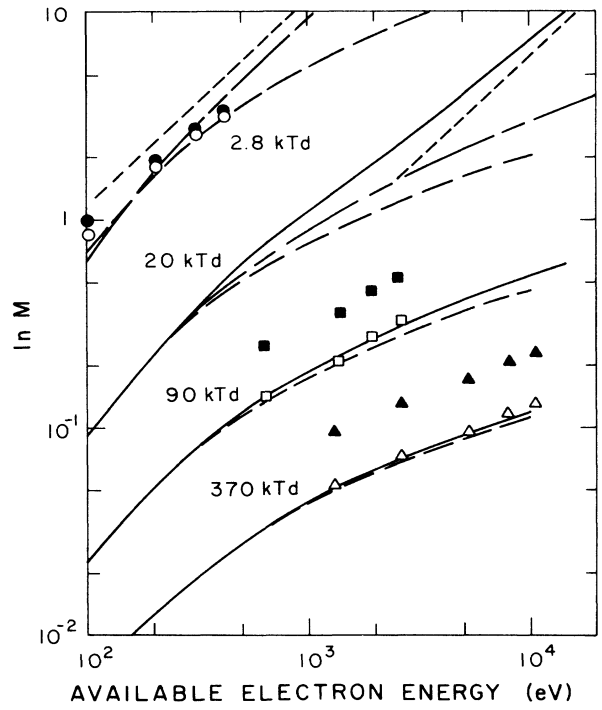

FIG. 3. Comparison of multiplication factors vs available energy as calculated using various models for electrons in Ar. The solid points are from Ref. 13 and include repeated backscattering. The open points are the single pass values calculated from the data shown by the solid points as discussed in the text. The solid, chain, and dashed curves are for single-beam models using the momentum-balance, energy-balance, and free-fall approximations, respectively. The short dashed lines are exponential growth curves calculated using the energy-balance approximation.

At intermediate E/n we have compared the three single-beam approximations at 20 kTd. In this case only the momentum-balance model approaches an exponential growth in the range of ε_a shown. At this E/n the multiple beam model with free fall shown by short dashed line, Eq. (15), gives an ionization coefficient of about $\frac{2}{3}$ of that for the single-beam momentum balance model. This comparison shows that the single-beam, energy-loss, and the free-fall models seriously underestimate the ionization at larger nz. The single-beam, momentum-loss and multibeam, free-fall models appear more realistic.

As predicted from the type of plot shown in Fig. 1, the free-fall and energy-balance models at 2.8 kTd agree surprisingly well up to about 400 eV of available energy, but the momentum balance gives $M = 0$ because the electron energy never reaches the ionization potential. On the other hand, the energy balance calculations yield a straight line (exponential growth) for energies above about 300 eV and differ from experiment[26] (short dashed line) by only 20%.

C. Steady-state ionization coefficients

Steady-state ionization coefficients characterizing the spatial growth of electron density in N_2 calculated using some of the models of Sec. II are shown in Fig. 4 along with experimental data. The single link chain curve is calculated using the multiple-beam, energy-balance model,[27] i.e., Eq. (14) and Eq. (6) without the ionization-growth term. This model is equivalent to that first used by Friedland and Kagan.[5] Their results are shown by the open points. The double and triple link chain curves were calculated using either Eq. (5) or Eq. (6) in Eq. (10), i.e., the single-beam, energy- and momentum-balance models, respectively. The short dashed curve shows the results of recent two-term spherical harmonic calculations.[12]

The curves and data of Fig. 4 show that our multiple-beam, energy-balance model[27] gives excellent agreement with the experiments of I for E/n from 800 to 7000 Td. Note that for $E/n > 1500$ Td the results of the multiple-beam, energy-balance and multiple-beam, free-fall models are the same. From Fig. 1 we see that this E/n is just above that at which energy runaway can occur. We

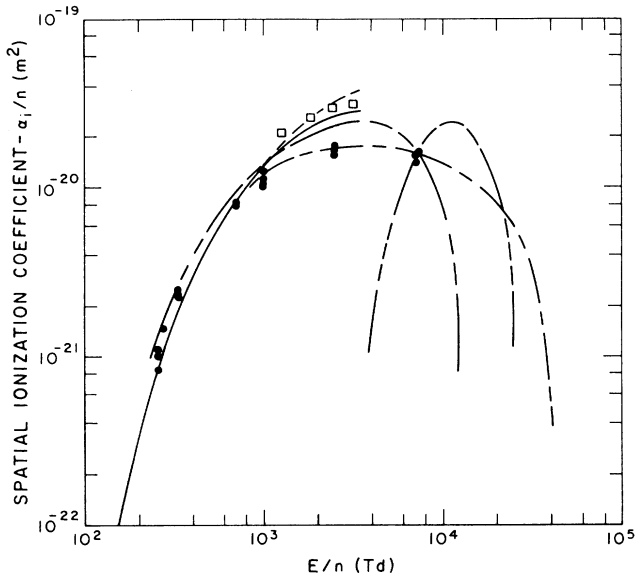

FIG. 4. Comparison of steady-state spatial ionization coefficients vs E/n from experiment and calculations using various models for electrons in N_2. The solid curve is an average of published experiments, while the solid points are from paper I. The short dashed curves are from theory using the two-term spherical harmonic expansion. The single short link chain curve is from the multiple-beam model using the energy balance. The double and triple short link curves are from the single-beam models using the energy- and momentum-balance approximations.

propose that the large calculated ionization coefficients of Friedland and Kagan[5] for N_2 are the result of their choice of parameters which result in too large an ionization cross section for N_2.

As pointed out in I, an understanding of the discrepancy between the two experimentally determined ionization coefficients awaits better experiment and theory. Electron reflection from the anode as discussed in I and spatially dependent secondary emission from the cathode[15] may be important here. The single-beam, energy-balance model yields ionization coefficients which are within about 50% of experiment for E/n from 250 to 10 000 Td, and so at least serves as a very simple and useful first approximation. The single-beam, momentum-balance model is useful for calculation of steady-state ionization coefficients only in a limited range of E/n. From these comparisons we conclude that the single-beam, energy-balance model is a good compromise between simplicity and accuracy, but that the multiple-beam, energy-balance model gives a better fit to the experimental data of I. A further example of the greater utility of the models based on the energy balance rather than the momentum balance is shown by the better agreement with experimental measurements of 391.4-nm emission from N_2 in Fig. 11 of I.

D. Electron backscattering and maximum range

In this section we illustrate the calculation of electron backscattering and then use the same procedure to calculate the maximum range of low-energy electrons for comparison with the experimental data. The electron energy versus distance was calculated using Eq. (20). The apparent ionization or excitation was then calculated using Eqs. (9) and (10). The upper curves of Fig. 5 show the calculated apparent ionization coefficients for reflected electrons with energies ε_r of 1 keV and 100 eV in Ar at $E/n = 42.6$ kTd plotted as a function of density times distance from the anode. This distance is measured from the right-hand side of the graph so as to simulate the experimental plots in which the anode is at the right. For the 1-keV case the ionization by electrons leaving the anode is indicated by the dashed curve, while that by electrons returning to the anode are indicated by the chain curve. The solid curve is the sum of these contributions. We again note that the behavior of the ionization curve is similar to that expected for allowed excitation processes, e.g., the ion lines of Ar (Ref. 28) or dissociative excitation of N_2 (Ref. 29). The lower curves are for electron excitation of the 811.5-nm line[30] of Ar, which is the strongest emission line observed in recent experiments in our laboratory.[2]

The left-hand portion of Fig. 5 shows the calculated apparent ionization and excitation coefficients for 100-eV electrons in Ar. Note the different normalized distance scales for the 100-eV and 1-keV electrons. In the case of ionization by 100-eV backscattered electrons, the ionization-coefficient curves for leaving and returning

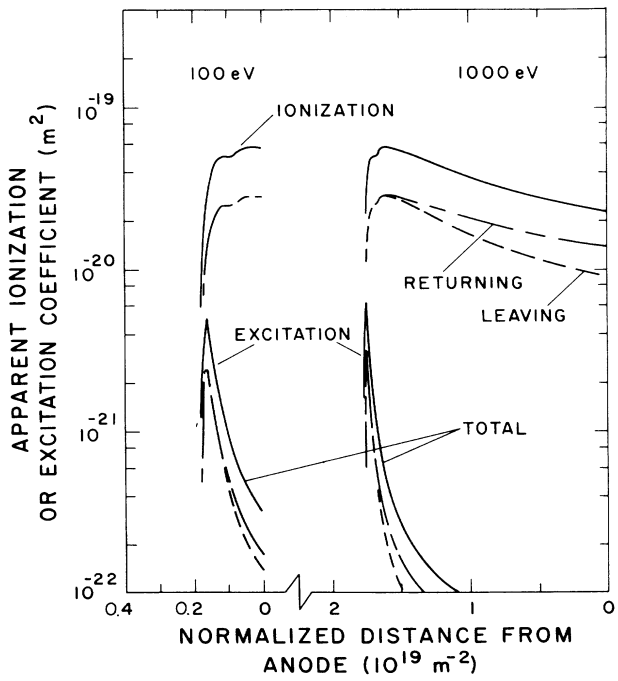

FIG. 5. Apparent ionization and excitation coefficients vs distance from anode time density for backscattered electrons in Ar with initial energies of 100 and 1000 eV. Here $E/n = 42.6$ kTd and opposes the motion of the electrons. The dashed and chain curves show the ionization and excitation produced by electrons leaving and returning to the anode, while the solid curves show their sums.

electrons are not distinguishable. It is recognized that the spatial distributions of ionization and excitation calculated using this beam model in which the electron trajectories are undeflected by collisions will greatly overestimate the fraction of the electrons reaching the larger distances from their point of origin.[25] It is expected, however, that when the large spread of initial energy and angle of backscattered electrons from the anode is incorporated, the result will be realistic spatial distribution. In any case, these calculations give a good indication of the maximum distance from the anode at which one can expect to observe the effects of backscattered electrons of various energies.

A closely related calculation and measurement is that of maximum electron range. It is also the only test of the slowing-down calculations for low initial energy electrons which we have found. We therefore compare the range of low-energy electrons with measurements of the maximum or extrapolated range of such electrons.[31–34] This comparison is shown in Fig. 6 where the solid points show measured values and the smooth curves are the distances at which the electron energy drops below the ionization or excitation energy appropriate to the particular gas and experiment. The calculations were made using Eq. (20) with $E/n=0$ and omitting the ionization-growth term $\varepsilon Q_0^i(\varepsilon)$. In this case ε_r is the energy with which the electrons are injected into the gas. The short dashed curve is the theory-based correlation of Grün for relatively high-energy electrons.[34] The calculated values are within about 30% of the experimental data. We note that one reason for discussing these results in this paper is the previously discussed[35] correlation between the slowing down of moderate-energy electrons in regions of low electric field known as the negative glow.

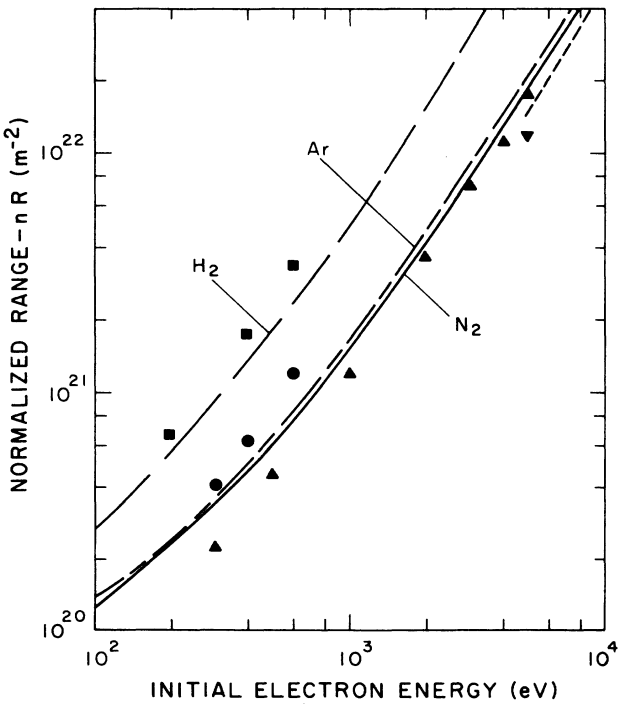

FIG. 6. Comparison of calculated and measured values of the extrapolated range of low-energy electrons in various gases. The labeled smooth curves are our calculated values. The short dashed curve is from Grün (Ref. 34). The gases, symbols and references are H_2—■—31; Ar—●—31; N_2—▼—32; N_2—▲—33.

IV. SUMMARY

We have shown that very simple beam models of electron motion in a gas give useful predictions of spatially dependent ionization and excitation coefficients at very high E/n. We find that use of the single-beam treatment of ionization rather than the multiple-beam treatment changes calculated spatially dependent ionization coefficients for H_2 by less than a factor of 2. The use of the free-fall approximation for electron motion is found to be valid over most of the E/n range considered in previous Monte Carlo calculations for Ar. We find that beam models based on the electron-energy balance agree better with more detailed models and with experiment than do beam models based on the momentum balance, particularly at lower E/n. The multiple-beam treatment of ionization and the use of the energy balance give ionization coefficients for N_2 at $E/n > 800$ Td in good agreement with the experimental results of I, but below previously published values at $E/n=3000$ Td. The single-beam, energy-balance model is used to describe the slowing down and reacceleration of electrons backscattered from the anode. When it is used to calculate the maximum range of electrons slowing down in various gases in the absence of an electric field, the results agree with experiment to within 30% for electron energies for which data are available.

Although the comparisons presented in this paper are limited to a uniform electric field, it is worth noting that with the exception of Eqs. (13)–(19), all equations apply equally well to nonuniform fields. The simple analytical forms in Eqs. (13)–(19) are based on Müller's[8] summations over individual beams who follow their parent's histories. The multiple-beam formulation derived by Friedland[5] was specifically for nonuniform fields, and the summations in that work are approximate.

Further evaluation of these models should be made when more detailed calculations utilizing three-moment,[10,21] Monte Carlo, or Boltzmann techniques and including anisotropic electron scattering become available. In the meantime, it would be of interest to extend these models to numerical simulations of electron behavior in the nonuniform electric fields present, for example, in the cathode fall of electric discharges.

ACKNOWLEDGMENTS

The authors would like to acknowledge helpful discussions with H. A. Blevin, A. Gallagher, P. Segur, and S. S. Yu. The work of two of us (A.V.P. and B.M.J.) was supported in part by the Lawrence Livermore National Laboratories, the Sandia National Laboratories, and the U.S. Air Force Office of Scientific Research. The work of the other (L.C.P.) was supported in part by Sandia National Laboratories.

*Also at Quantum Physics Division, National Bureau of Standards, Boulder, CO 80303 and Physics Department, University of Colorado, Boulder, CO 80309.

†Present and permanent address: Institute of Physics, P.O. Box 75, YU-11001, Belgrade, Yugoslavia.

[1]B. M. Jelenković and A. V. Phelps, *preceding paper,* Phys. Rev. A **36**, 5310 (1987).

[2]B. M. Jelenković and A. V. Phelps, in *Swarm Studies and Inelastic Electron-Molecule Collisions,* edited by L. C. Pitchford, B. V. McKoy, A. Chutjian, and S. Trajmar (Springer-Verlag, New York, 1985); B. M. Jelenković and A. V. Phelps, Bull. Am. Phys. Soc. **31**, 152 (1986); A. V. Phelps and B. M. Jelenković, *ibid.* **32**, 1143 (1987).

[3]G. W. Stuart and E. Gerjuoy, Phys. Rev. **119**, 892 (1960); E. Gerjuoy and G. W. Stuart, Phys. Fluids **3**, 1008 (1960); L. D. Pearlstein and G. W. Stuart, *ibid.* **4**, 1293 (1961).

[4]W. Briggs and S. S. Yu, Lawrence Livermore National Laboratory Report No., UCID-19399, 1982 (unpublished).

[5]L. Friedland, J. Phys. D **7**, 2246 (1974); L. Friedland and Yu. M. Kagan, *ibid.,* **15**, 1721 (1982); J. Appl. Phys. **54**, 4947 (1983); J. Phys. D **19**, 1019 (1986).

[6]R. Lagushenko and J. Maya, J. Appl. Phys. **55**, 3293 (1984).

[7]A. V. Gurevich, Zh. Eksp. Teor. Phys. **39**, 1296 (1960) [Sov. Phys.—JETP **12**, 904 (1960)]; Usp. Fiz. Nauk. **120**, 319 (1976) [Sov. Phys.—Usp. **19**, 869 (1976)]; **132**, 685 (1980) [**23**, 862 (1980)].

[8]G. Ecker and K. G. Müller, Z. Naturforsch. **16a**, 246 (1961); K. G. Müller, Z. Phys. **169**, 432 (1962); K. G. Müller and W. O. Müller, Z. Naturforsch. **30a**, 1553 (1975).

[9]J. H. Ingold, in *Gaseous Electronics, Electrical Discharges,* edited by M. N. Hirsch and H. J. Oskam (Academic, New York, 1978), Vol. I, pp. 36–38.

[10]K.-U. Riemann, Bull, Am. Phys. Soc. **31**, 160 (1986).

[11]L. C. Pitchford, T. J. Moratz, P. Segur, and M. Yousfi, in *Swarm Studies and Inelastic Electron-Molecule Collisions,* by L. C. Pitchford, V. B. McCoy, A. Chutjain, and S. Trajmar (Springer-Verlag, New York, 1985), p. 115; see also P. Segur, M. Yousfi, and M. C. Bordage, J. Phys. D **17**, 2199 (1984).

[12]A. V. Phelps and L. C. Pitchford, Phys. Rev. A **31**, 2932 (1985).

[13]A. B. Parker and P. C. Johnson, Proc. R. Soc. London, Ser. A **325**, 511 (1971); J. D. Pace and A. B. Parker, J. Phys. D **6**, 1525 (1973); D. Bhasavanich and A. B. Parker, Proc. R. Soc. London, Ser. A **358**, 385 (1977). The M values from Pace and Parker for $E/n > 2.8$ kT appear to us to be much too low.

[14]K. D. Granzow and G. W. McClure, Phys. Rev. **125**, 1792 (1962).

[15]M. A. Folkhard and S. C. Haydon, Aust. J. Phys. **23**, 847 (1970).

[16]Y. Sakai, H. Tagashira, and S. Sakamoto, J. Phys. B **5**, 1010 (1972); N. Sato and H. Tagashira, J. Phys. D **18**, 2451 (1985).

[17]M. Hayashi, *Proceedings of the 4th IEE Conference on Gas Discharges* (Institute of Electrical Engineers, London, 1976), p. 195.

[18]E. J. Lauer, S. S. Yu, and D. M. Cox, Phys. Rev. **23**, 2250 (1981).

[19]T. Moratz, L. C. Pitchford, and J. N. Bardsley, J. Appl. Phys. **61**, 2146 (1987).

[20]T. Holstein, Phys. Rev. **70**, 367 (1946); W. P. Allis, *Electron Emission. Gas Discharges I,* Vol. 21, of *Handbuch der Physik* (Springer, Berlin, 1956), p. 421.

[21]Y. M. Li and L. C. Pitchford (unpublished).

[22]A. J. Dempster, Phys. Rev. **46**, 728 (1934).

[23]B. Brockelhurst and F. A. Downing, J. Chem. Phys. **46**, 2976 (1967).

[24]K. Kumar, H. R. Skullerud, and R. E. Robson, Aust. J. Phys. **33**, 343 (1980).

[25]R. C. Smith, Appl. Phys. Lett. **25**, 292 (1974).

[26]J. Dutton, J. Phys. Chem. Ref. Data **4**, 577 (1975).

[27]The calculations for this model are not shown for $E/n < 800$ Td because of numerical inaccuracies in the integration.

[28]P. N. Clout and D. W. O. Heddle, J. Phys. B **4**, 483 (1971).

[29]J. F. M. Aarts and F. J. De Heer, Physica **52**, 45 (1971); M. J. Mumma and E. C. Zipf, J. Chem. Phys. **55**, 5582 (1971).

[30]J. K. Ballou, C. C. Lin, and F. E. Fajen, Phys. Rev. A **8**, 1797 (1973).

[31]J. F. Lehmann, Proc. R. Soc. London **115**, 624 (1927).

[32]A. Cohn and G. Caledonia, J. Appl. Phys. **41**, 3767 (1970).

[33]J. L. Barret and P. B. Hays, J. Chem. Phys. **64**, 743 (1976).

[34]A. E. Grün, Z. Naturforsch. **12a**, 89 (1957).

[35]M. J. Druyvesteyn and F. M. Penning, Rev. Mod. Phys. **12**, 87 (1940); G. Francis, *Gas Discharges II,* Vol. 22 of *Handbuch der Physik* (Springer, Berlin, 1956), p. 81.